Partially Coherent Quantum Models for Human Two-Choice Decisions

Ian G. Fuss
School of Electrical and Electronic Engineering
University of Adelaide, SA 5005, Australia

Daniel J. Navarro
School of Psychology
University of Adelaide, SA 5005, Australia

Abstract

Psychological models for two-choice decision tasks typically model the probability that a particular response is made at time t via the first-passage time to an absorbing boundary for some stochastic process. In contrast to the most commonly used models which use classical random walks for the underlying process, a recent paper by Busemeyer, Wang, & Townsend (2006) proposed that quantum walks may provide an interesting alternative. In this paper, we extend this work by introducing a class of *partially-coherent quantum walk models* that can be applied to human two-choice tasks. The models trace out a path from quantum to classical models, preserving some of the desirable features of both. We discuss the properties of these models, and the potential implications for modeling simple decisions.

Introduction

The hypothesis that human induction and decision-making can exploit quantum mechanical phenomena is one that has a great deal of intuitive appeal. Perhaps the currently most famous and controversial version of this hypothesis is Penrose's (1989) suggestion that mathematical insight relies on quantum mechanical effects. Although a number of aspects of that specific version of the hypothesis are controversial (see Searle 1997), there remains a certain face validity to the more general idea. In particular, one of the most basic findings from quantum computing is that it is possible to exploit the parallelism inherent in quantum mechanics to speed up a number of computational problems (Shor 1994, 1997; Grover 1997). Since human decision processes unfold over time, it is plausible to suggest that an evolutionary advantage would accrue to decision-makers that can make effective use of quantum mechanical effects. Of course, many questions need to be answered before we can determine with confidence whether or not this advantage has in fact been achieved by living organisms. Indeed, at least four important scientific perspectives have significant bearing on these questions, namely those of psychology, biology, computer science and physics (see Litt *et al.* 2006, for instance). This paper is concerned primarily with a psychological perspective but makes use of insights from the other three disciplines.

From the psychological perspective, one of the main issues with which we must be concerned is the construction of formal models that make predictions about human behaviour. That is, if the brain can make use of quantum phenomena in its processing, or (in a weaker formulation) obeys dynamical laws that reflect the mathematical structure of quantum mechanics, what patterns would one expect to observe in human behaviour? In this paper, we adopt the weaker "functionalist" perspective, and consider psychological models that use quantum mechanical principles. The stronger claim, that human information processing genuinely makes use of quantum physical phenomena, is beyond the scope of this paper.

In a pioneering paper, Busemeyer, Wang, & Townsend (2006) explored the possibility of a formal characterisation of human decision making processes based on quantum mechanical principles. Their model was constructed as a quantum mechanical analogue of a standard random walk model (e.g., Stone 1960) for human decisions and decision latencies. They found that this quantum mechanical model could reproduce some of the basic findings in the literature on human decision-making. In this paper we extend this work in two respects. Firstly, we consider a more general quantum walk that has its origins in computer science and physics (Aharonov, Davidovich, & Zagury 1993; Meyer 1996). We cast this quantum walk into a linear systems framework (Fuss *et al.* 2007) that allows us to demonstrate the similarities to and differences from a classical random walk. Secondly, we employ a density matrix formalisation of the walk, allowing us to extend the quantum walk framework to accommodate the influence of noise on the evolution of the walk. This second aspect produces *partially-coherent quantum walk models*, which subsume both classical and quantum walks as special cases. When high levels of noise are injected into the walk, the quantum state decoheres completely, and the model reduces to a Bernoulli random walk. When the noise levels are set to zero, we obtain a pure quantum walk model. As a result, we arrive at a model for human decision making that allows us to infer the extent to which quantum behaviour is manifest.

The structure of this paper is as follows. In the first section, we introduce two walk processes, one classical and one quantum, and discuss their interpretations as linear systems. We then discuss the use of absorbing boundaries as psychological decision criteria, and the calculation of the first passage time distributions for both processes. Having

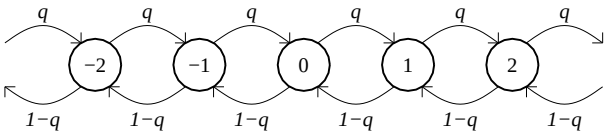

Figure 1: The transition diagram for a Bernoulli random walk. Each node corresponds to a possible location x for the walk, and each link is labelled by the amount of probability mass that transfers between locations at each time point.

constructed these special cases, we then introduce the more general partially-coherent walks, and discuss three plausible noise processes. Finally, we provide a brief discussion of the behaviour of the first passage time distributions for partially-coherent walks, as a function of the amount and type of noise involved.

Sequential Sampling Models, Classical and Quantum

Our approach, like that of Busemeyer, Wang, & Townsend (2006), is based on a general class of sequential sampling models commonly used to describe human evidence-accrual and decision-making (e.g., Ratcliff & Smith 2004). The central assumption of such models is that the environment provides people only with noisy stimulus representations, and so to make accurate decisions people draw successive samples from this representation until some *decision threshold* is reached. This class of models (see, e.g., Ratcliff 1978; Vickers 1979; Smith & van Zandt 2000) draws heavily from sequential analysis (Wald 1947) and stochastic processes (Smith 2000), and is at present the best formal framework available for modeling decision accuracy, latency, and subjective confidence in simple decision tasks.

Bernoulli Random Walks

The simplest kind of sequential sampling model relies on Bernoulli sampling in discrete time. At each time point, the observer accrues a single piece of evidence drawn from a Bernoulli distribution: with probability q, the evidence favors response A, and with probability $1 - q$ it favors response B. The observer draws samples until some decision threshold is reached; typically, when the number of samples favoring one option exceeds the number of samples favoring the other option by some fixed amount. A procedure of this kind defines a discrete random walk on the line, taking a step up with probability q and a step down with probability $1 - q$. Commonly, one applies a variant of the so-called "assumption of small steps" (see Luce 1986) and takes the limit to a continuous Wiener diffusion model (Feller 1968; Ratcliff 1978). For conceptual simplicity, however, we retain the original Bernoulli model.

Formally, in the discrete Bernoulli random walk, we consider the evolution of the probability distribution $p(x, t) \in \mathbb{R}$

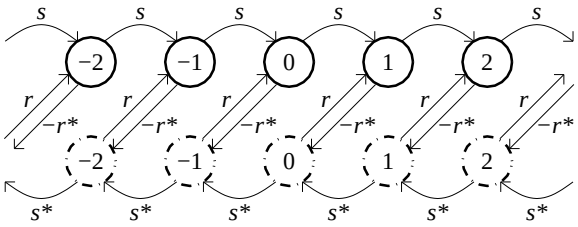

Figure 2: The transition diagram for a two-state quantum walk. Each node corresponds to one element of the state vector, with the top row corresponding to the right-handed elements, and the bottom row to the left-handed elements. Each node is labelled with its location x. The coefficients r, r^*, s and s^* refer to the amount of probability amplitude that transfers between different elements (in this illustration, we set $k = 0$ for simplicity).

for discrete times $t \geq 0$, and possible locations $x \in \mathbb{Z}$, from an initial distribution over locations $p(x, 0)$. The dynamics of this walk evolve according to the linear difference equation

$$p(x, t + 1) = qp(x - 1, t) + (1 - q)p(x + 1, t), \qquad (1)$$

where $q \in [0, 1]$. The transition diagram for this difference equation is given in Figure 1, and illustrates how the probability mass is transferred between successive time points. Since it is a linear system, Equation 1 can be written in the matrix form

$$\boldsymbol{p}(t + 1) = \mathbf{M}\boldsymbol{p}(t), \qquad (2)$$

where the transpose of the probability state vector is

$$\begin{aligned} \boldsymbol{p}^{\mathsf{T}}(t) \quad = \quad & (\ldots p(-2, t), p(-1, t), p(0, t), \\ & p(1, t), p(2, t), \ldots), \end{aligned} \qquad (3)$$

and the one-step time evolution matrix is

$$\mathbf{M} = \begin{bmatrix} \cdot & \cdot & \cdot & \cdot & \cdot & \cdot \\ \cdot & 0 & 1-q & 0 & 0 & \cdot \\ \cdot & q & 0 & 1-q & 0 & \cdot \\ \cdot & 0 & q & 0 & 1-q & \cdot \\ \cdot & 0 & 0 & q & 0 & \cdot \\ \cdot & \cdot & \cdot & \cdot & \cdot & \cdot \end{bmatrix}. \qquad (4)$$

Note that the columns of $\mathbf{M}$ sum to 1, so as to preserve the constraint that probabilities sum to 1 at all times (i.e., isometry).

Although it is somewhat unnecessary for Bernoulli walks, since analytic expressions exist for most of their interesting psychological properties (Feller 1968), this kind of matrix formulation is very useful in general. As discussed by Diederich & Busemeyer (2003), adopting simple matrix representations for evidence accrual processes serves a useful pragmatic goal, insofar as it simplifies the subsequent calculation of model predictions in those cases where analytic expressions do not exist.

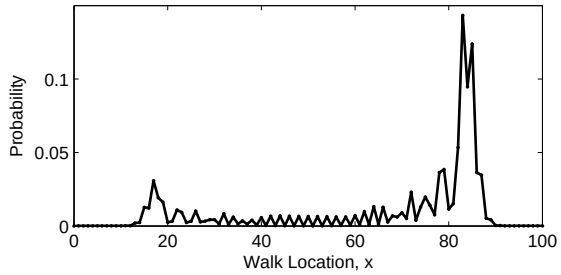

Figure 3: The distribution of a Hadamard walk, measured at $t = 50$. The initial state of the walk places probability amplitude $1/2$ for both chiralities at the location $x = 50$, and amplitude $1/2\sqrt{2}$ at both chiralities for $x = 49$ and $x = 51$ (essentially an analogue of the Bernoulli case with probability 1/2 in the middle location, and 1/4 on either side).

Quantum Walks

The Bernoulli random walk is a classical model: it traces out a single path on the line. However, in a quantum system there is an inherent parallelism, insofar as (in the absence of measurement) the evidence-accrual process now traces out multiple paths simultaneously. Consequently, the variance of a quantum walk increases quadratically with time in contrast to a linear increase of the variance for a Bernoulli random walk. Hence we would expect a quantum decision maker to make decisions considerably faster than the corresponding classical decision maker. In this section, we describe the basic quantum walk model.

Quantum walks differ from classical ones in two main respects: firstly, although the dynamics are still linear, they are described with respect to probability amplitudes (complex numbers whose squared absolute values sum to 1), not probabilities (real numbers that sum to 1); and secondly in order to preserve isometry on the probabilities, the operator must be unitary. Unitarity imposes strong constraints on the kinds of dynamics that may be considered, and as a consequence, quantum walks in which the particle has only a *location* $x \in \mathbb{Z}$ are extremely uninteresting. Typically, this is addressed by allowing the particle to have a *chirality* (left or right) as well as a location. The state of the walk at time t is then described by the spinor

$$\boldsymbol{\psi}(x,t) = \begin{pmatrix} \psi_R(x,t) \\ \psi_L(x,t) \end{pmatrix}, \tag{5}$$

where $\psi_R(x,t) \in \mathbb{C}$ is a complex-valued scalar that describes the probability amplitude in state x with right-chirality at time t. A natural analogue of the Bernoulli walk for this system involves some probability amplitude moving from the location x to the locations $x+1$ or $x-1$, but with the chirality changing as well. More precisely, the dynamics of the state evolve according to the difference equations (Aharonov, Davidovich, & Zagury 1993; Meyer 1996)

$$\psi_R(x,t+1) \quad = \quad e^{ik}\left[s\psi_R(x-1,t) + r\psi_L(x-1,t)\right]$$

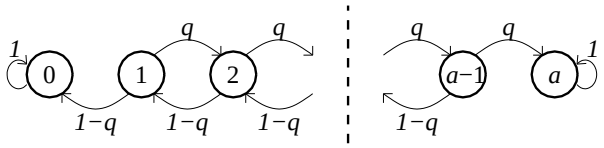

Figure 4: The transition diagram for an absorbing boundary random walk. The structure differs from that in Figure 1 only in that the states $x = 0$ and $x = 1$ do not send probability mass to other states: instead, all probability mass is preserved in the self-transition links at each end of the diagram.

$$\psi_L(x,t+1) \quad = \quad e^{ik}\left[-r^*\psi_R(x+1,t) + s^*\psi_L(x+1,t)\right], \tag{6}$$

where $|r|^2 + |s|^2 = 1$, s^* is the complex conjugate of s, and $k \in \mathbb{R}$. The structure of this walk is illustrated by the transition diagram in Figure 2, which describes the one-step evolution for the probability amplitudes, in the case where $k = 0$. Notice that the coefficient s controls the probability amplitude that stays in the same chirality, with amplitudes in the left chirality consistently moving leftward (i.e., x decreases), and amplitudes in the right chirality moving right (x increases). The coefficient r controls the "reversal" of the chirality from left to right and vice versa. In order to illustrate the basic characteristics of this kind of quantum walk, Figure 3 shows what happens when a so-called "Hadamard walk" (where $e^{ik} = i$ and $s = r = i/\sqrt{2}$) is evolved for 50 time steps and then measured.

Decisions and First Passage Times

The development so far describes an evidence-accrual process that (be it classical or quantum mechanical) evolves without constraint on $x \in \mathbb{Z}$. Psychologically, however, since x is interpreted as an evidence value, and time is of the essence to the decision-maker, it is generally assumed that once x hits either 0 or a, the evidence-accrual terminates and a decision is made. Accordingly, both 0 or a act as *absorbing boundaries*, and the decision latency is described by the *first passage time distribution* to the boundaries.

Bernoulli Random Walks

Not surprisingly, the classical case is straightforward: in order to calculate the first passage times to absorbing boundaries at $x = 0$ and $x = a$ we modify the Bernoulli random walk to have the transition diagram shown in Figure 4. The nodes at $x = 0$ and $x = a$ will thus contain the cumulative distribution of absorbed particles at a given time. Since we are interested in first passage times it is convenient to relax the requirement that $\mathbf{M}$ produce an isometry by dropping the self-transitions on the end nodes. They will then contain the first passage time probability for that time. If we choose

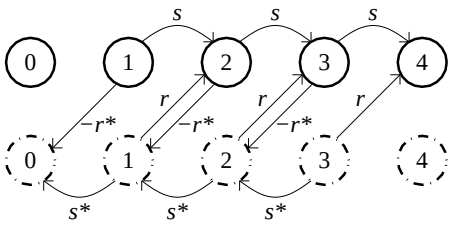

Figure 5: The transition diagram for a quantum walk with absorbing boundaries, in which we set $a = 4$, and remove the self-transition edges. In all other respects, the transition structure mimics the one in Figure 2.

$a = 4$ then the one step time evolution matrix is

$$\mathbf{M} = \begin{bmatrix} 0 & 1-q & 0 & 0 & 0 \\ 0 & 0 & 1-q & 0 & 0 \\ 0 & q & 0 & 1-q & 0 \\ 0 & 0 & q & 0 & 0 \\ 0 & 0 & 0 & q & 0 \end{bmatrix}. \quad (7)$$

The model is completed by a choice of the initial state such as

$$\boldsymbol{p}^{\mathsf{T}}(0) = (0, 0, 1, 0, 0). \quad (8)$$

Hence, $p(0, t)$ is the first passage time distribution for the $x = 0$ boundary and $p(4, t)$ is the first passage time distribution for the $x = 4$ boundary.

Quantum Walks

The absorbing boundary problem for quantum walks is a little more subtle. We define the projection operators

$$\mathbf{P}_e = |x \leq 0\rangle \langle x \leq 0| \quad (9)$$
$$\mathbf{P}_f = |0 < x < a\rangle \langle 0 < x < a| \quad (10)$$
$$\mathbf{P}_c = |a \leq x\rangle \langle a \leq x|, \quad (11)$$

where $\mathbf{P}_e$ projects from the Hilbert space containing the spinors $\boldsymbol{\psi}$ onto its subspace with support $[-\infty, 0]$ and similarly $\mathbf{P}_f$ projects onto the subspace with support $(0, a)$ and $\mathbf{P}_c$ projects onto the subspace with support $[a, \infty]$. We consider the problem where at each time t we make partial measurements of the quantum walk with the operators $\mathbf{P}_e$ and $\mathbf{P}_c$. This effectively modifies the time evolution process described by the transition diagram in Figure 2 to one described by transition diagrams such as that in Figure 5, where we have chosen the case where $a = 4$ for simplicity.

We can write a matrix equation

$$\boldsymbol{\psi}_{4c}(t + 1) = \mathbf{U}_{4c}\boldsymbol{\psi}_{4c}(t) \quad (12)$$

for the operations described by this transition diagram, where

$$\begin{aligned} \boldsymbol{\psi}_{4c}^{\mathsf{T}}(t) = (&\psi_R(0, t), \psi_L(0, t), \psi_R(1, t), \psi_L(1, t), \\ &\psi_R(2, t), \psi_L(2, t), \psi_R(3, t), \psi_L(3, t), \\ &\psi_R(4, t), \psi_L(4, t)), \end{aligned} \quad (13)$$

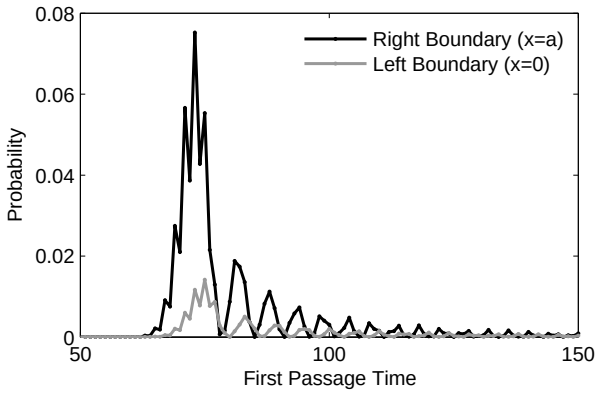

Figure 6: First passage times to the two boundaries (with $a = 100$) for the Hadamard walk in Figure 3.

and the one-step time evolution matrix is

$$\mathbf{U}_{4c} = e^{ik} \begin{bmatrix} 0 & 0 & 0 & 0 & 0 & 0 & 0 & 0 & 0 & 0 \\ 0 & 0 & -r^* & s^* & 0 & 0 & 0 & 0 & 0 & 0 \\ 0 & 0 & 0 & 0 & 0 & 0 & 0 & 0 & 0 & 0 \\ 0 & 0 & 0 & 0 & -r^* & s^* & 0 & 0 & 0 & 0 \\ 0 & 0 & s & r & 0 & 0 & 0 & 0 & 0 & 0 \\ 0 & 0 & 0 & 0 & 0 & 0 & -r^* & s^* & 0 & 0 \\ 0 & 0 & 0 & 0 & s & r & 0 & 0 & 0 & 0 \\ 0 & 0 & 0 & 0 & 0 & 0 & 0 & 0 & 0 & 0 \\ 0 & 0 & 0 & 0 & 0 & 0 & s & r & 0 & 0 \\ 0 & 0 & 0 & 0 & 0 & 0 & 0 & 0 & 0 & 0 \end{bmatrix}. \quad (14)$$

We complete the matrix specification by defining an initial state

$$\begin{aligned} \boldsymbol{\psi}_{4c}^{\mathsf{T}}(0) = (&c_R(0), c_L(0), c_R(1), c_L(1), c_R(2), c_L(2), \\ &c_R(3), c_L(3), c_R(4), c_L(4)). \end{aligned} \quad (15)$$

The first passage time distributions to the two boundaries are then obtained by making the partial measurements corresponding to observation of the two absorbing states at each time point,

$$p(0, t) = |\psi_R(0, t)|^2 + |\psi_L(0, t)|^2 \quad (16)$$
$$p(4, t) = |\psi_R(4, t)|^2 + |\psi_L(4, t)|^2. \quad (17)$$

So, for instance, the first passage time distributions for a Hadamard walk (see Figure 3) can be easily computed, and are illustrated in Figure 6.

Partially Coherent Quantum Walks

Since in psychology we are rarely confronted with pure systems of any kind, we would like to allow for the possibility that our quantum walks decohere as a result of their interaction with their environment. Decoherence is one pathway from quantum to classical systems so we expect our walks to produce the quantum walk results for low decoherence and the random walk results for high decoherence.

We formulate the partially coherent quantum walk in terms of density matrices $\boldsymbol{\rho}(x, t)$. The density matrix representation for a quantum state is constructed by taking the

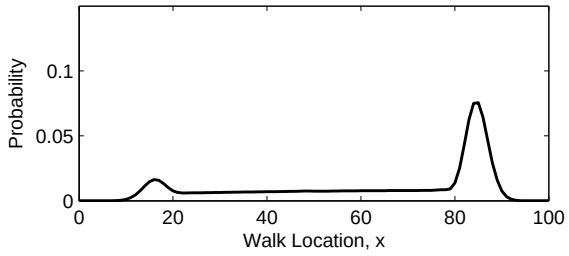

Figure 7: The distribution of a free Hadamard walk (at $t = 50$) with a small amount of phase damping ($\alpha = 0.1$), and a Gaussian distribution over start points (suitably discretised, with mean $x = 50$ and standard deviation 5).

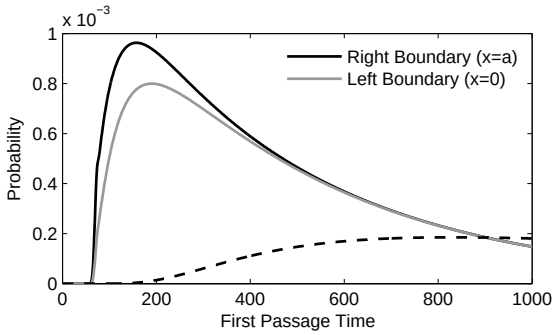

Figure 8: First passage times to the two boundaries (with $a = 100$) for a phase-damped Hadamard walk with a moderate amount of noise ($\alpha = 0.5$). The dashed line shows the corresponding first passage time for the fully-decoherent case where $\alpha = 1.0$ (i.e., a Bernoulli walk).

outer product of the spinor and its adjoint,

$$\boldsymbol{\rho}(x, x', t) = \boldsymbol{\psi}(x, t)\boldsymbol{\psi}^{\dagger}(x', t). \tag{18}$$

Thus the ij-th cell of the density matrix $\rho_{ij}(x, x', t)$ is simply the product $\psi_i(x, t)\psi_j^*(x, t)$. Accordingly, the main diagonal elements of $\boldsymbol{\rho}$ are real-valued and non-negative, and describe the probabilities (not amplitudes) associated with a particular state. The "correlations" between the states are represented by the off-diagonal elements of the matrix, which are complex-valued.

When adopting the density matrix formulation, we begin by constructing the initial state from the spinor, as follows:

$$\boldsymbol{\rho}(x, x', 0) = \boldsymbol{\psi}(x, 0)\boldsymbol{\psi}^{\dagger}(x', 0). \tag{19}$$

We then inject noise into the density matrix before applying the time evolution operator $\mathbf{U}$. If we let $\tilde{\boldsymbol{\rho}}(x, x', t)$ denote a noise-corrupted density matrix at time t, then the evolution of the system is described by,

$$\boldsymbol{\rho}(x, x', t + 1) = \mathbf{U}\tilde{\boldsymbol{\rho}}(x, x', t)\mathbf{U}^{\dagger}, \tag{20}$$

and we inject noise once more to arrive at $\tilde{\boldsymbol{\rho}}(x, x', t + 1)$, the noise-corrupted density matrix at time $t + 1$. In order to include absorbing boundaries at each stage we make partial measurements of the noisy density matrix. In the example with boundaries at $x = 0$ and $x = 4$ to obtain the first passage time probabilities at each time step we measure

$$p(0, t) = \rho_{0,0}(0, 0, t) + \rho_{1,1}(0, 0, t) \tag{21}$$

and

$$p(4, t) = \rho_{0,0}(4, 4, t) + \rho_{1,1}(4, 4, t), \tag{22}$$

noting that in doing so we collapse the first two and last two columns and rows of the density matrix, in analogy with the coherent case state functions.

Noise Processes

In the previous discussion, we were non-specific as to how noise should be introduced into the pure quantum system. In fact, there are a number of plausible candidates for psychological noise processes, and *a priori* it is difficult to choose between them. Therefore, we have chosen to discuss three possibilities (see Nielsen & Chuang 2000 for a broader discussion), each of which describes a way of calculating $\tilde{\boldsymbol{\rho}}$ from $\boldsymbol{\rho}$. In all cases, the basic approach is to apply noise operators $\mathbf{E_0}, \mathbf{E_1}, \ldots, \mathbf{E}_m$ to the density matrix $\boldsymbol{\rho}$, such that

$$\tilde{\boldsymbol{\rho}}(x, x', t) = \sum_{j=0}^{m} \mathbf{E}_j \boldsymbol{\rho}(x, x', t)\mathbf{E}_j^{\dagger}. \tag{23}$$

It is worth noting the noise and time-evolution operators can be seen as two aspects to a single "noisy evolution". That is, by putting Equations 20 and 23 together, we can directly describe the time evolution of the system using

$$\tilde{\boldsymbol{\rho}}(x, x', t + 1) = \mathbf{U}\left(\sum_{j=0}^{m} \mathbf{E}_j \tilde{\boldsymbol{\rho}}(x, x', t)\mathbf{E}_j^{\dagger}\right)\mathbf{U}^{\dagger}. \tag{24}$$

Phase damping. The main noise process we will consider is *phase damping*, a process that has been the subject of much study and speculation. Of import to us is its candidacy for the process responsible for the world around us appearing classical. The operator formalism for phase damping uses the following two matrices;

$$\mathbf{E}_0 = \begin{bmatrix} 1 & 0 \\ 0 & \sqrt{1-\alpha} \end{bmatrix} \tag{25}$$

$$\mathbf{E}_1 = \begin{bmatrix} 0 & 0 \\ 0 & \sqrt{\alpha} \end{bmatrix}, \tag{26}$$

where for notational convenience $\mathbf{E}_0$ and $\mathbf{E}_1$ are written for a two state system. For larger systems, we construct block diagonal matrices using these elements: for instance, $\mathbf{E}_0$ would be constructed by placing copies of the matrix in Equation 25 along the diagonal, and inserting zeros everywhere else. Since this means that only the main diagonal and alternating elements of the first upper and lower diagonals can be non-zero, the noise process in our walk has direct influence only on the chirality, not the location.

One of the first things to note about phase damping noise is that a little noise goes a long way, particularly when

combined with uncertainty about the start point. Figure 7 shows the state of mildly phased-damped Hadamard walk ($\alpha = 0.1$) at time $t = 50$, in which the initial distribution $\boldsymbol{p}(0)$ is Gaussian, with mean $x = 50$ and standard deviation 5. The overall shape is very similar to the pure walk illustrated in Figure 3, but the high-frequency oscillations have all been smoothed out, leaving a simple bimodal distribution. In short, a small amount of noise suffices to remove the most psychologically-implausible multimodalities in the walk.

The second observation to note is that, while a small amount of noise introduces a lot of smoothing, large changes to the first-passage time distributions are noticeable even with a substantial amount of decoherence. To illustrate this, Figure 8 plots the first passage time distributions for $\alpha = 0.5$ against the corresponding fully-decoherent case ($\alpha = 1.0$; equivalent to a Bernoulli walk). Even at moderate to large amounts of noise, the partially-coherent walk achieves a substantial speed-up relative to its classical counterpart.

Amplitude damping. The second type of noise we consider is *amplitude damping*, and we discuss two distinct varieties. The first version arises when a quantum system is coupled with the vacuum, and is referred to as *spontaneous decay*. The operator formalism for amplitude damping via spontaneous decay is

$$\mathbf{E}_0 = \begin{bmatrix} 1 & 0 \\ 0 & \sqrt{1-\alpha} \end{bmatrix} \quad (27)$$

$$\mathbf{E}_1 = \begin{bmatrix} 0 & \sqrt{\alpha} \\ 0 & 0 \end{bmatrix}. \quad (28)$$

An example of amplitude damping is given in Figure 9. As with the previous phase-damped example, a moderate amount of noise has been injected into the walk. In this case, however, the resulting first passage times are bimodal at the right boundary, illustrating that the partially-coherent walk can produce some predictions that are qualitatively different in character to the Bernoulli walk. The figure also illustrates the fact that one needs to take care when making claims about the characteristics of such processes: this plot is based on a (non-Hadamard) quantum walk that is in fact symmetric in the absence of noise.

The more general version involves decay to a thermal system rather than to the vacuum. The operators for generalised amplitude damping are,

$$\mathbf{E}_0 = \sqrt{p}\begin{bmatrix} 1 & 0 \\ 0 & \sqrt{1-\alpha} \end{bmatrix} \quad (29)$$

$$\mathbf{E}_1 = \sqrt{p}\begin{bmatrix} 0 & \sqrt{\alpha} \\ 0 & 0 \end{bmatrix} \quad (30)$$

$$\mathbf{E}_2 = \sqrt{1-p}\begin{bmatrix} \sqrt{1-\alpha} & 0 \\ 0 & 1 \end{bmatrix} \quad (31)$$

$$\mathbf{E}_3 = \sqrt{1-p}\begin{bmatrix} 0 & 0 \\ \sqrt{\alpha} & 0 \end{bmatrix}. \quad (32)$$

This noise model applies to systems where relaxation processes couple the quantum system to a system that is in thermal equilibrium at a temperature that is generally much higher than the quantum system. A useful physical analogy for brain processes decaying via this mechanism is that of nuclear magnetic resonance quantum computation where the spin states relax via T_1 processes coupling them to their surrounding lattice.

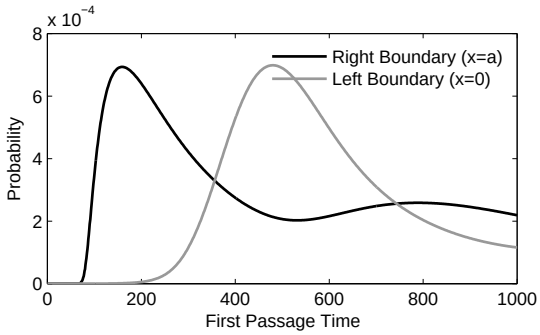

Figure 9: First passage times to the two boundaries (with $a = 100$) for an amplitude-damped ($\alpha = 0.2$) walk with $k = 0$, $r = -i/\sqrt{2}$ and $s = 1/\sqrt{2}$.

Depolarisation. Our final noise type is *depolarisation*. Though we do not discuss it in detail, this kind of noise is illustrative of noise models considered by quantum communication and computing research. The operator formalism for depolarisation relies on the following four matrices,

$$\mathbf{E}_0 = \sqrt{1-\frac{3\alpha}{4}}\begin{bmatrix} 1 & 0 \\ 0 & 1 \end{bmatrix} \quad (33)$$

$$\mathbf{E}_1 = \sqrt{\frac{\alpha}{4}}\begin{bmatrix} 0 & 1 \\ 1 & 0 \end{bmatrix} \quad (34)$$

$$\mathbf{E}_2 = \sqrt{\frac{\alpha}{4}}\begin{bmatrix} 0 & i \\ -i & 0 \end{bmatrix} \quad (35)$$

$$\mathbf{E}_3 = \sqrt{\frac{\alpha}{4}}\begin{bmatrix} 1 & 0 \\ 0 & -1 \end{bmatrix}. \quad (36)$$

The second ($\mathbf{E}_1$) and last ($\mathbf{E}_3$) operators correspond to *qubit bit flip* and *phase flip* errors respectively while the middle one is a combination of the two. It is interesting to note that phase flip noise is equivalent to phase damping noise.

The Behaviour of Partially-Coherent Walks

As discussed previously, our primary aim in this paper is to extend the psychological theory developed by Busemeyer, Wang, & Townsend (2006), and illustrate how injecting noise into the walk gives rise to partially-coherent walks that preserve the desirable characteristics of their classical counterparts, while retaining some of the interesting properties of the pure quantum walks. While the psychological theory is not as-yet fully developed, it is worth discussing the kinds of empirical data patterns that the partially-coherent walks are able to capture. To illustrate this, the left panels of Figure 10 show the first passage time distributions for a phase-damped Hadamard walk at several different levels of noise, while the right panels show the corresponding dis-

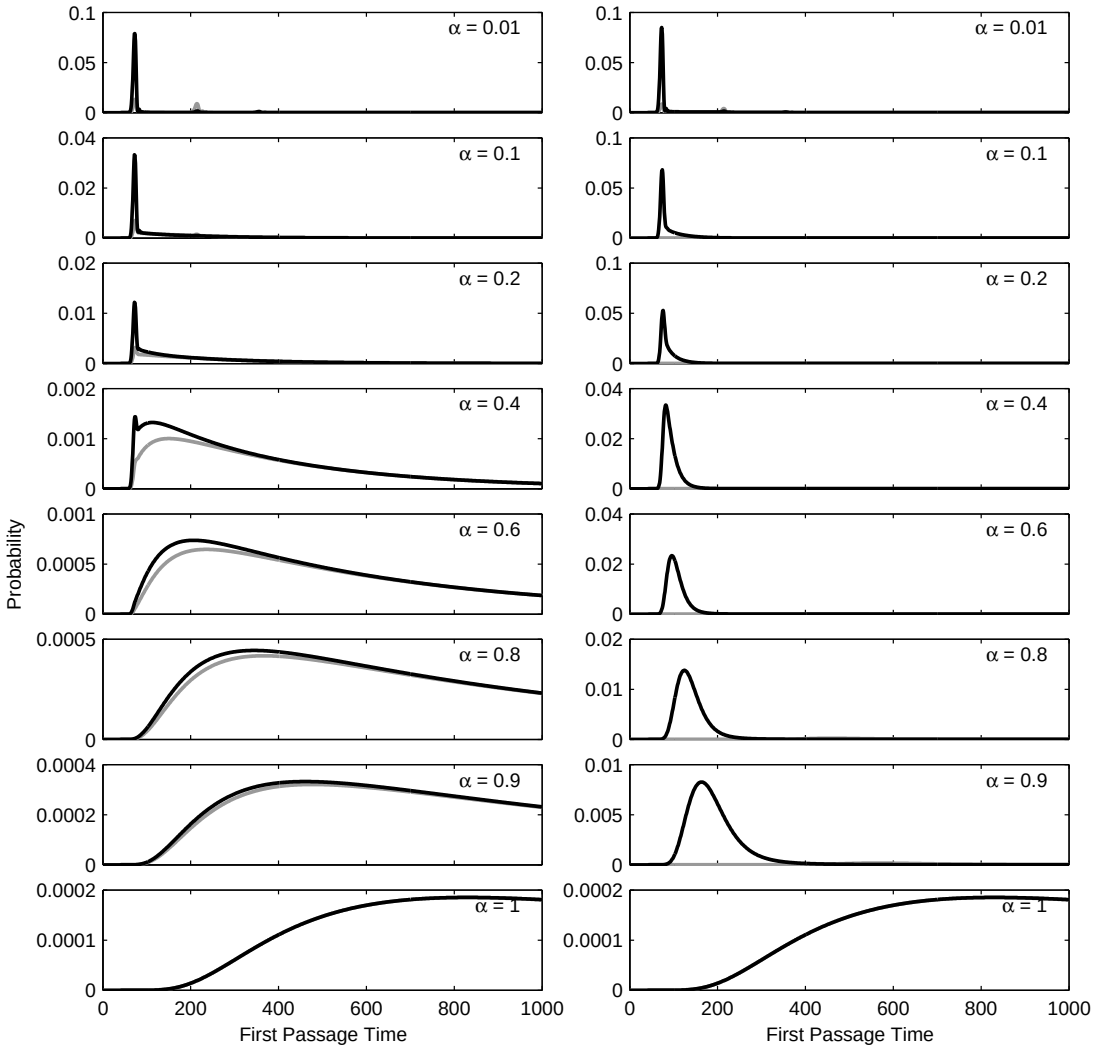

Figure 10: The effect of adding noise to a Hadamard walk with $a = 100$. On the left-hand side, phase-damping noise is added to the walk, whereas on the right, the noise is amplitude-damping. The level of the noise increases from top to bottom; the noise levels α are 0.01, 0.1, 0.2, 0.4, 0.6, 0.8, 0.9 and 1.0. In all plots, the first passage time distributions are shown over the range $0 \leq t \leq 1000$. As with previous figures, the black line plots the first passage times to the right boundary $x = a$, and the grey line plots hitting times for the left boundary $x = 0$. In the uppermost panel, the noise levels are high enough to smooth out the interference patterns in Figure 6, but low enough for "quantum tunnelling" effects to be observed, in which the absorbing boundaries become partially reflecting, leading to a second mode appearing much later than the first.

tributions for an amplitude-damped walk. Notice that the two noise processes have different effects on the distributions: phase-damping approaches classical behaviour much faster, and in doing so suppresses the asymmetry of the Hadamard walk, since the first passage distributions converge. In contrast, while amplitude-damping approaches classical behaviour more slowly, it suppresses drift to the left boundary.

Discussion

Sequential sampling models are at present the best formal framework available for modeling accuracy, latency, and confidence in simple decisions. In Gigerenzer & Todd's (1999) terms, they make reasonable assumptions about how people gather evidence (*information search*), when they stop (*termination rules*), and what decision is then made (*decision rule*). However, while this framework places some constraints on what kinds of models are admissable, it still allows considerable variation in the low-level details; some

evidence-accrual models are continuous (Ratcliff 1978) and others discrete (Smith & van Zandt 2000). Variation in termination rules also exists, with a distinction made between accumulator (Vickers 1979) and random walk models.

In their recent paper (Busemeyer, Wang, & Townsend 2006) demonstrate that, in addition to these existing issues, psychological evidence-accrual based on quantum walks needs to be considered alongside its classical counterpart. One method to accommodate this issue is to consider more general models that trace out a path from the purely quantum to purely classical, in much the same way that competitive accumulators can move from random walk to accumulator behaviour (Usher & McClelland 2001). Such models would exhibit a broad spectrum of behaviours that correspond to quantum systems of varying degrees of coherence.

In this paper we have developed exactly such a class of models, including subclasses corresponding to different types of decoherence-inducing noise. Of particular note is that partially-coherent quantum systems produce first passage time distributions that often have shapes similar to classical walks, but predict much faster response times. This indicates that inference from human reaction data for or against the possibility of quantum or quantum like processes giving rise to human behaviour is more subtle than previously envisaged. In part, this subtlty arises from the inherent complexity associated with inverting the reaction time profiles to obtain the underlying evidence gathering processes (the well-known model mimicry problem; e.g., Ratcliff & Smith 2004). The bimodal shapes of the noisy Hadamard walks, for example, are quite different from the unimodal shape of the Bernoulli walk, yet the two often produce similarly shaped first-passage time distributions. Nevertheless, a number of the shapes in Figures 9 and 10 are quite distinct from the classical distributions, providing (among other things) one possible avenue for explaining the bimodal response time distributions that are sometimes observed.

One final issue bears mentioning: besides the potential value in enabling research into the extent to which the mind satisfies quantum mechanical principles, partially-coherent walks tie into a long-standing issue in response time modeling, namely the extent to which evidence accrues serially or in parallel (see, e.g., Townsend & Ashby 1983). In quantum walks evidence accrual occurs in parallel, whereas classical walks are serial. One interesting line of work would be to make explicit connections to existing serial-parallel discussions.

Acknowledgments Correspondence concerning this article should be addressed to Ian Fuss, School of Electrical and Electronic Engineering, University of Adelaide, e-mail: ifuss@eleceng.adelaide.edu.au. The second author was supported by an Australian Research Fellowship (ARC project DP-0773794).

References

Aharonov, Y.; Davidovich, L.; and Zagury, N. 1993. Quantum random walks. *Phys. Rev. A.* 48:1687–1690.

Busemeyer, J. R.; Wang, Z.; and Townsend, J. T. 2006. Quantum dynamics of human decision-making. *Journal of Mathematical Psychology* 50:220–241.

Diederich, A., and Busemeyer, J. 2003. Simple matrix methods for analyzing diffusion models of choice probability, choice response time and simple response time. *Journal of Mathematical Psychology* 47:304–322.

Feller, W. 1968. *An Introduction to Probability Theory and its Applications*. New York: Wiley.

Fuss, I.; White, L. B.; Sherman, P.; and Naguleswaran, S. 2007. Analytic views of quantum walks. *Proc. Of SPIE, Noise and Fluctuations in Photonics, Quantum Optics and Communications* 6603.

Gigerenzer, G., and Todd, P. M. 1999. *Simple heuristics that make us smart*. Oxford: Oxford University Press.

Grover, L. K. 1997. Quantum mechanics helps in searching for a needle in a haystack. *Phys. Rev. Lett.* 79:325.

Litt, A.; Eliasmith, C.; Kroon, F. W.; Weinstein, S.; and Thagard, P. 2006. Is the brain a quantum computer? *Cognitive Science* 30:593–603.

Luce, R. D. 1986. *Response Times: Their Role in Inferring Elementary Mental Organization*. New York, NY: Oxford University Press.

Meyer, D. A. 1996. From quantum cellular automata to quantum lattice gases. *Journal of Statistical Physics* 85:551–574.

Nielsen, M. A., and Chuang, I. L. 2000. *Quantum Computation and Quantum Information*. Cambridge, UK: Cambridge University Press.

Penrose, R. 1989. *The Emperor's New Mind: Concerning Computers, Minds and the Laws of Physics* . Oxford Unversity Press.

Ratcliff, R., and Smith, P. L. 2004. A comparison of sequential sampling models for two-choice reaction time. *Psychological Review* 111:333–367.

Ratcliff, R. 1978. A theory of memory retrieval. *Psychological Review* 85:59–108.

Searle, J. R. 1997. *The Mystery of Consciousness* . Granta.

Shor, P. W. 1994. Algorithms for quantum computation: discrete logarithms and factoring. In Goldwasser, S., ed., *Proceedings of the 35th Annual Symposium on Foundations of Computer Science* , 124–134. Los Alamitos, CA: IEEE Press.

Shor, P. W. 1997. Polynomial time algorithms for prime factorisation and discrete logarithms on a quantum computer. *SIAM J. Comp.* 26:1484–1509.

Smith, P. L., and van Zandt, T. 2000. Time dependent poisson counter models of response latency in simple judgment. *British Journal of Mathematical and Statistical Psychology* 53:293–315.

Smith, P. L. 2000. Stochastic dynamic models of response times and accuracy: A foundational primer. *Journal of Mathematical Psychology* 44:408–463.

Stone, M. 1960. Models for choice reaction time. *Psychometrika* 25:251–260.

Townsend, J. T., and Ashby, F. G. 1983. *Stochastic Modeling of Elementary Psychological Processes* . Cambridge, UK: Cambridge University Press.

Usher, M., and McClelland, J. L. 2001. The time course of perceptual choice: The leaky, competing accumulator model. *Psychological Review* 108:550–492.

Vickers, D. 1979. *Decision Processes in Visual Perception* . New York, NY: Academic Press.

Wald, A. 1947. *Sequential Analysis*. New York: Wiley.